Isotope production in spallation reaction of ^{93}Zr and ^{93}Nb induced by proton and deuteron

Keita NAKANO[†1]

[1]J-PARC Center, Japan Atomic Energy Agency, Tokai-mura, Ibaraki 319-1195, Japan
[†]Email: nakano.keita@jaea.go.jp

Abstract

Nuclear transmutation technology has been attracting attention as a method for treating high-level radioactive waste. One of the candidates is the spallation reaction using high-energy particles, especially for the nuclides with relatively small neutron-capture cross sections such as long-lived fission product (LLFP) ^{93}Zr. The accumulation of nuclear reaction data and the development of nuclear reaction models based on the data are indispensable for the accurate prediction of the amount of conversion of ^{93}Zr to stable nuclides and/or short-lived nuclides and residual long-lived nuclides after the transmutation. Therefore, under the ImPACT program (Period: 2014 − 2018), we have measured isotope-production cross sections in proton- and deuteron-induced spallation reactions on LLFP ^{93}Zr and adjacent nuclide ^{93}Nb at RIKEN RIBF. In the experiment, a ^{93}Zr beam at 50 MeV/nucleon and a ^{93}Nb beam at 113 MeV/nucleon were produced by inflight-fission of ^{238}U. These beams were irradiated to secondary targets containing hydrogen and deuterium to induce spallation reactions, and the product yields were analyzed by ZeroDegree Spectrometer to determine the product cross sections. The results are compared with the nuclear reaction models.

1 Introduction

The problem of the high-level radioactive waste disposal is one of the most important issues in the nuclear energy field. In order to reduce the long-term risk of the high-level radioactive waste, research and development of transmutation technologies have been carried out. However, while the transmutation of minor actinoids has been studied by fast reactors and accelerator-driven nuclear transmutation systems [1], the transmutation of long-lived fission products (LLFPs), which also have a long-term risk, has not been widely studied. Therefore, transmutation studies of the LLFPs with half-lives longer than 100,000 years were conducted in the ImPACT program [2]. Among the LLFPs, ^{93}Zr has a very long half-life of 1.5 million years and a relatively high fission yield of approximately 6%. On the other hand, since ^{93}Zr has a relatively smaller neutron-capture cross section than other long-lived fission products [3], it was necessary to explore a new method other than transmutation using a nuclear reactor. Therefore, transmutation of ^{93}Zr by spallation reactions using high-energy protons and deuterons has been proposed. In order to evaluate the performance of this method, isotope-production cross sections for proton- and deuteron-induced reactions on ^{93}Zr, which are the most important data to estimate the amount of transmutation and the radioactivity after irradiation activity, are required.

In this study, we measured the isotope-production cross sections of 50 MeV/nucleon proton and deuteron bombardment on ^{93}Zr in order to improve nuclear reaction models which will be used for the study of the LLFP transmutation. The newly measured data are also useful to discuss the energy dependence of the isotope-production cross sections by combining with

experimental data at 105 and 209 MeV/nucleon [4, 5]. In addition, we measured the isotope-production cross sections in 113-MeV/nucleon proton- and deuteron-induced reactions on ^{93}Nb. The proton and neutron numbers in ^{93}Nb are $Z = 41$ and $N = 52$, respectively, whereas they are $Z = 40$ and $N = 53$ in ^{93}Zr. It is interesting to see how the difference of a single nucleon in the initial proton and neutron numbers influences the reproducibility of the nuclear reaction models by comparing the results with the previous ^{93}Zr data at 105 MeV/nucleon [4].

2 Experiment

Both the ^{93}Zr and ^{93}Nb experiments were performed at the RIKEN Radioactive Isotope Beam Factory (RIBF) using a cocktail beam containing secondary beams of ^{93}Zr and ^{93}Nb. Since the experimental procedures and setups for the ^{93}Zr and ^{93}Nb experiments were similar, only the details of the ^{93}Zr experiments will be described here.

In the ^{93}Zr experiment, the BigRIPS [6] and the ZeroDegree Spectrometer (ZDS) [6] were used to analyze secondary beams and reaction products, respectively. First, a ^{238}U primary beam accelerated up to 345 MeV/nucleon impinged onto a 7-mm-thick ^{9}Be primary target installed at the entrance of BigRIPS. The secondary beam containing ^{93}Zr ions was produced through inflight-fission of the ^{238}U primary beam. The secondary beam was identified using beamline detectors placed in the second-half of the BigRIPS. Then the secondary beam impinged onto a secondary target, cooled gaseous H_2 and D_2 [7], at the entrance of the ZDS. The residual nuclei produced in the nuclear reactions with the secondary targets were also identified by beamline detectors at ZDS. Seven different magnetic-field settings $\Delta(B\rho)/B\rho = -6\%$, -4%, -2%, 0%, $+2\%$, $+4\%$, and $+6\%$ were adopted to measure wide ranges of mass numbers and charge states of the reaction products. The typical current of the primary beam was approximately 400 enA.

3 Data Analysis

Same as the experimental procedure, since the main procedures of the data analysis of the ^{93}Zr and ^{93}Nb experiments are almost the same, the data analysis only for the ^{93}Zr will be presented here.

Particle identification of the secondary beam was performed based on the TOF$-B\rho-\Delta E$ method [8] using signals from the beamline detectors. Left panel of Figure 1 shows a two-dimensional identification plot of the secondary beam by the atomic number Z and the mass-to-charge ratio A/Q. As shown in the left panel of Figure 1, the secondary beam contains only isotones of ^{93}Zr. Each nuclide was clearly separated with resolutions of 0.45 (FWHM) in Z and 0.28 (FWHM) in A, which are sufficient to identify the ^{93}Zr beam. The events in the ranges $39.6 \leq Z \leq 40.4$ and $2.319 \leq A/Q \leq 2.333$ were selected as the ^{93}Zr beam. The purity, which is calculated as a ratio of the number of ^{93}Zr beam in the above-mentioned ranges to the number of total events, and the typical count rate of ^{93}Zr were 57.8% and 980 counts per second, respectively. The energy of the ^{93}Zr beam were 51 and 52 MeV/nucleon at the centers of the H_2 and D_2 targets, respectively, calculated from the magnetic rigidity of the secondary beam before the secondary target considering the energy loss in beamline materials using the LISE++ code [9]. The energy spreads in the secondary targets were calculated as $\pm$10 MeV/nucleon.

Same as the particle identification of secondary beam, that of the reaction products was performed based on the TOF$-B\rho-\Delta E$ method. Right panel of Figure 1 indicates the identification plot of the reaction products from the H_2 secondary target at the 0% ZDS $B\rho$ setting after selecting the ^{93}Zr beam.

The isotope-production cross sections were determined from the number of incident ^{93}Zr ions and the number of each isotope. A systematic uncertainty was estimated to be 4.6% including

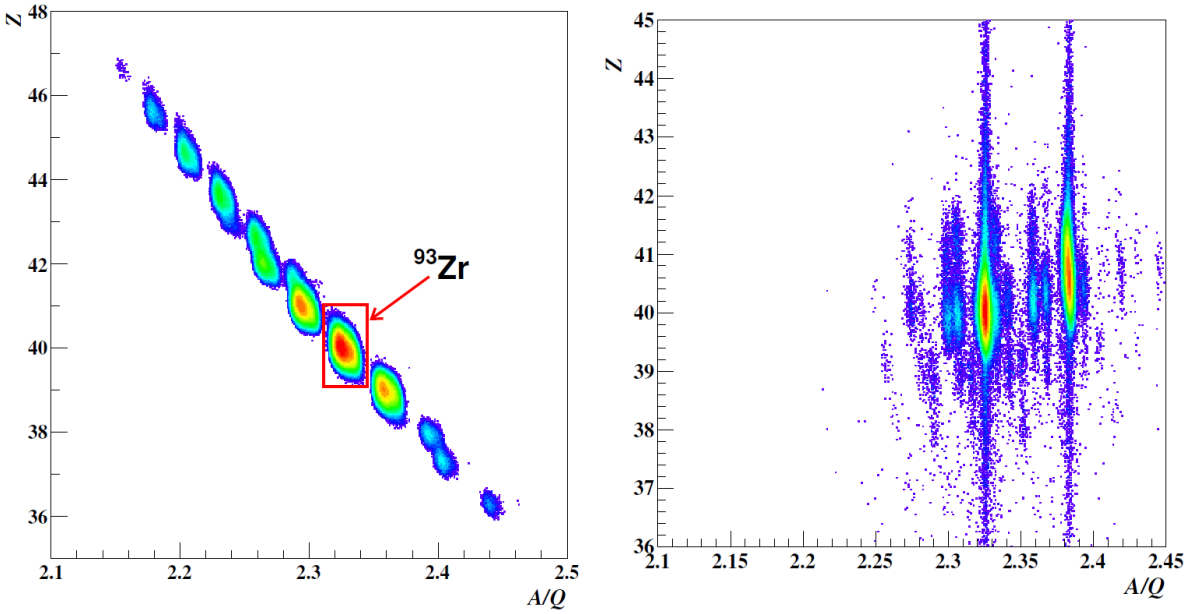

Figure 1: Left: Particle identification plot of the secondary beam by the atomic number Z and the mass-to-charge ratio A/Q in the ^{93}Zr experiment. Right: Particle identification plot of the reaction product from the H_2 secondary target after selecting the ^{93}Zr beam in the 0% $B\rho$ setting.

uncertainties of the thickness of the secondary target, multiple reactions in the secondary target, and the energy spread in the secondary target.

4 Results and Discussion on ^{93}Zr data

Figure 2 shows the measured isotope-production cross sections in the proton- and deuteron-induced reactions on ^{93}Zr at 50 MeV/nucleon together with those at 105 and 209 MeV/nucleon [4, 5]. The black circles are the measured isotope-production cross sections in the proton case, and the red triangles in deuteron case. The black solid and red dashed lines correspond to calculated cross sections by PHITS [10] in the proton- and deuteron-induced reactions, respectively. The upper, middle, and lower panels show the data at 209, 105, and approximately 50 MeV/nucleon, respectively. The error bars include only the statistical uncertainties. Jumps at the neutron magic number $N = 50$, which is pointed out in the previous works [4, 5], are seen in the Zr-isotopic chain for both the proton- and deuteron-induced reactions and in the Y-isotopic chain for the deuteron-induced reaction even in the data at 50 MeV/nucleon. In the Y-isotopic chain, ^{87}Y has a noticeble large production cross section. This corresponds to the first peak of an excitation function of the ^{93}Zr$(p, x)^{87}$Y reaction around 50 MeV/nucleon.

The PHITS calculations are in good agreement with the measured data even with the newly measured data. In particular, the trend around ^{87}Y in the 51-MeV proton-induced reaction was successfully reproduced by the PHITS calculation. However, discrepancies as seen in the previous works are still observed in the data at 50 MeV/nucleon: one-mass-shifts to the heavy side in the distribution of the Nb-isotopic chain, underestimations of the production cross sections in the neutron-deficient region of Nb- and Y-isotopic chains, overestimations of the production cross sections near the target nucleus ^{93}Zr, and an exaggerated even-odd staggering in the Sr-isotopic chain. In terms of the energy dependence of the reproducibility of the PHITS calculations, the ratio of calculation to experimental (C/E) of the ^{92}Zr and ^{92}Y production cross

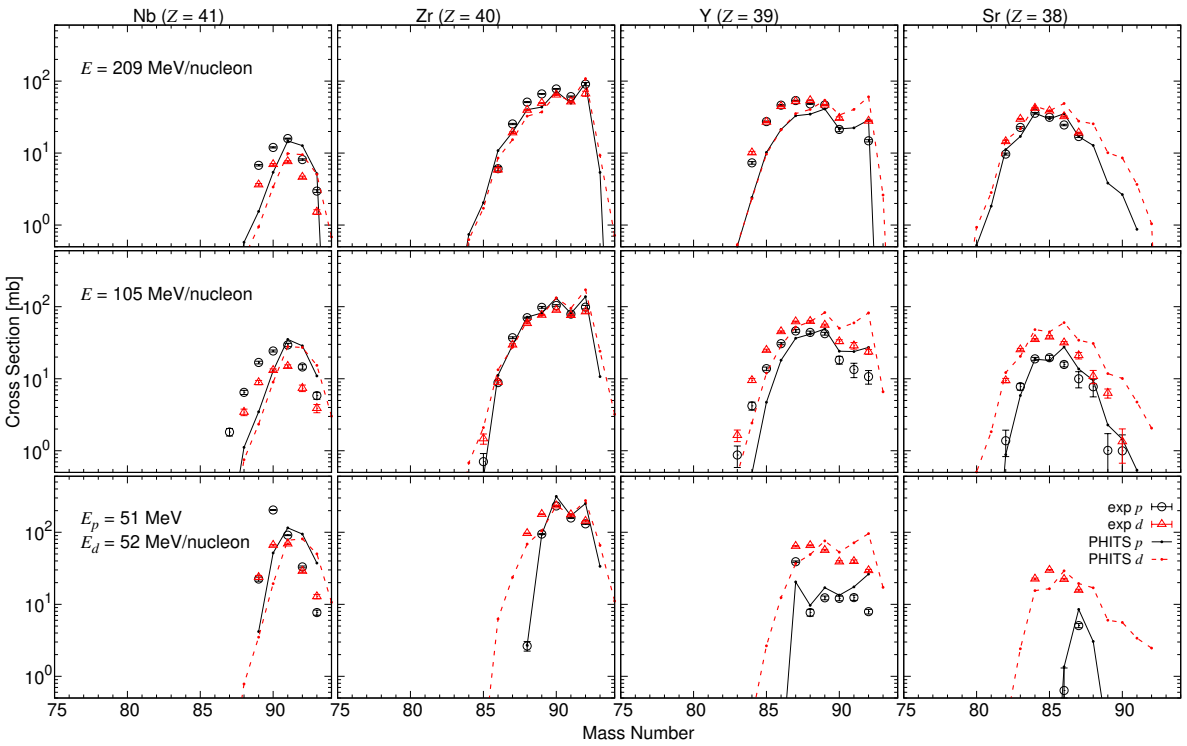

Figure 2: Isotope-production cross sections for the proton- and deuteron-induced reactions on ^{93}Zr.

sections are getting worse as the decrease of the incident energy in the proton-induced cases. In the deuteron-induced cases, on the other hand, the C/E of those have the largest value in the data at 105 MeV.

5 Results and Discussion on ^{93}Nb data

Figure 3 shows the measured isotope-production cross sections in the proton- and deuteron-induced reactions on ^{93}Nb at 113 MeV/nucleon. The black circles and red triangles correspond to the measured data in the proton- and deuteron-induced reactions, respectively. The PHITS calculations are also plotted by the black solid lines for the proton-induced case and by the red dashed lines for the deuteron-induced case. Although discontinuous jumps at the neutron magic number $N = 50$ are observed in the Zr-isotopic chains for both the proton- and deuteron-induced reactions because of the closed-shell structure, no clear jump appeared in the Nb-isotopic chain.

The PHITS calculations well reproduce the measured isotope-production cross sections as does the ^{93}Zr data. Also, the four discrepancies seen in the ^{93}Zr data are also found in the ^{93}Nb data. In particular, the underestimations of the production cross sections in the neutron-deficient region of the Nb- and Y-isotopic chains are observed for the both ^{93}Zr and ^{93}Nb data. If the atomic number of the target nuclide increases by one, it might be expected that the atomic number of the underestimated nuclide also increases by one, that is, cross sections of the Mo- and Zr-isotopic chains are expected to be underestimated in ^{93}Nb data. However, the underestimated isotopic chains remained the same for both ^{93}Nb and ^{93}Zr targets. This demonstrates that the reproducibility of the calculation is largely influenced by the final nuclides rather than the reaction.

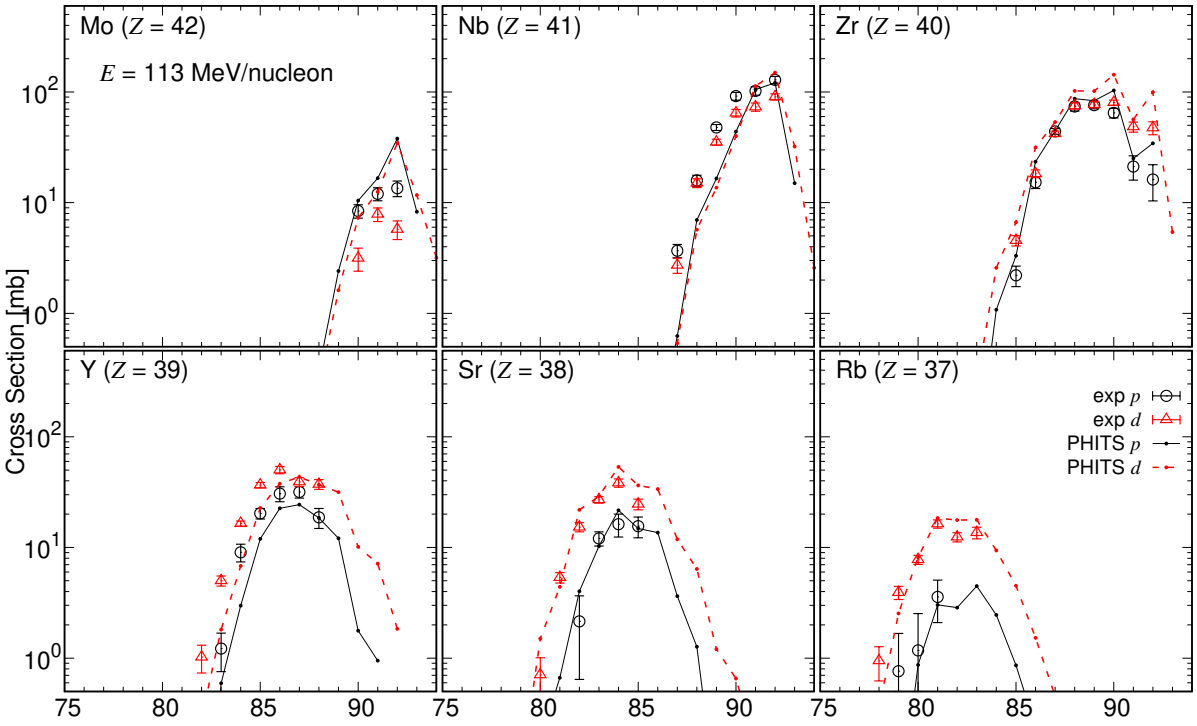

Figure 3: Isotope-production cross sections for the proton- and deuteron-induced reactions on ^{93}Nb.

6 Summary

Isotope-production cross sections for the proton- and deuteron-induced reactions on ^{93}Zr at approximately 50 MeV/nucleon and ^{93}Nb at 113 MeV/nucleon were measured at RIKEN RIBF. The measured data are useful to discuss the reaction energy and target nucleus dependences of the isotope-production cross sections. The comparison of the ^{93}Zr data at the three different reaction energies with the PHITS calculations revealed that the four discrepancies are identically seen in the isotope-production cross sections at the reaction energies ranging from 50 to 200 MeV/nucleon. In particular, the overestimations of the production cross sections near the target nucleus become more serious at the lower reaction energy. The comparison between the measred ^{93}Nb data and the PHITS calculations demonstrates that the discrepancies are observed despite the changes of the atomic and mass number by one. Also, the underestimations in the neutron deficient-region are seen in the Nb- and Y-isotopic chains for the both ^{93}Zr and ^{93}Nb data regardless of the difference of the atomic number of the target nuclei ^{93}Zr and ^{93}Nb.

References

[1] Tsujimoto K, Oigawa H, Ouchi N, et al. Research and Development Program on Accelerator Driven Subcritical System in JAEA. J Nucl Sci Technol. 2007;44(3):483-490.

[2] ImPACT Program. https://www.jst.go.jp/impact/program/08.html.

[3] Shibata K, Iwamoto O, Nakagawa T, et al. JENDL-4.0: A New Library for Nuclear Science and Engineering. J Nucl Sci Technol. 2011;48(1):1-30.

[4] Kawase S, Nakano K, Watanabe Y, et al. Study of proton- and deuteron-induced spallation reactions on the long-lived fission product ^{93}Zr at 105 MeV/nucleon in inverse kinematics. Prog Theor Exp Phys. 2017;2017:093D03.

[5] Kawase S, Watanabe Y, Nakano K, et al. Measurement of isotopic production cross sections of proton- and deuteron-indued reactions on ^{93}Zr at 200 MeV/nucleon. JAEA-Conf 2018-001. 2018;2018:111.

[6] Kubo T, Kameda D, Suzuki H, et al. BigRIPS separator and ZeroDegree spectrometer at RIKEN RI Beam Factory. Prog Theor Exp Phys. 2012;2012:03C003.

[7] Ryuto H, Kunibu M, Minemura T, et al. Liquid hydrogen and helium targets for radioisotope beams at RIKEN. Nucl Instrum Meth A. 2005;555:1-5.

[8] Fukuda N, Kubo T, Ohnishi T, et al. Identification and separation of radioactive isotope beams by the BigRIPS separator at the RIKEN RI Beam Factory. Nucl Instrum Meth B. 2013;317:323-332.

[9] Tarasov OB and Bazin D. LISE++: Exotic beam production with fragment separators and their design. Nucl Instrum Meth B. 2016;376:185-187.

[10] Sato T. Features of Particle and Heavy Ion Transport code System (PHITS) version 3.02. J Nucl Sci Technol. 2018;55:684-690.

Acknowledgments

I would like to thank ImPACT-RIBF collaborators for their contributions to the experiment, advice on data analysis, and fruitful discussion. I would like to thank the accelerator staff of the RIKEN Nishina center for providing high-quality ^{238}U primary beam. This works was funded by ImPACT Program of Council for Science, Technology and Innovation (Cabinet Office, Government of Japan).